Tracking plasma generated H2O2 from gas into liquid phase and revealing its dominant impact on human skin cells

Joern Winter, H. Tresp, M U Hammer, S. Iseni, S. Kupsch, A. Schmidt-Bleker, K. Wende, M. Dünnbier, K. Masur, K.-D. Weltmann, et al.

Journal of Physics D: Applied Physics

J. Phys. D: Appl. Phys. **47** (2014) 285401 (12pp) doi:10.1088/0022-3727/47/28/285401

Tracking plasma generated H_2O_2 from gas into liquid phase and revealing its dominant impact on human skin cells

J Winter[1,2], H Tresp[1,2], M U Hammer[1,2], S Iseni[1,2], S Kupsch[1,2], A Schmidt-Bleker[1,2], K Wende[1,2], M Dünnbier[1,2], K Masur[1,2], K-D Weltmann[2]and S Reuter[1,2]

[1] Centre for Innovation Competence plasmatis, Felix-Hausdorff-Str. 2, 17489 Greifswald, Germany
[2] Leibniz Institute for Plasma Science and Technology INP Greifswald e.V., Felix-Hausdorff-Str. 2, 17489 Greifswald, Germany

E-mail: winter@inp-greifswald.de

Received 2 March 2014, revised 14 May 2014
Accepted for publication 16 May 2014
Published 19 June 2014

Abstract

The pathway of the biologically active molecule hydrogen peroxide (H_2O_2) from the plasma generation in the gas phase by an atmospheric pressure argon plasma jet, to its transition into the liquid phase and finally to its inhibiting effect on human skin cells is investigated for different feed gas humidity settings. Gas phase diagnostics like Fourier transformed infrared spectroscopy and laser induced fluorescence spectroscopy on hydroxyl radicals ($^{\cdot}OH$) are combined with liquid analytics such as chemical assays and electron paramagnetic resonance spectroscopy. Furthermore, the viability of human skin cells is measured by Alamar Blue® assay. By comparing the gas phase results with chemical simulations in the far field, H_2O_2 generation and destruction processes are clearly identified. The net production rate of H_2O_2 in the gas phase is almost identical to the H_2O_2 net production rate in the liquid phase. Moreover, by mimicking the H_2O_2 generation of the plasma jet with the help of an H_2O_2 bubbler it is concluded that the solubility of gas phase H_2O_2 plays a major role in generating hydrogen peroxide in the liquid. Furthermore, it is shown that H_2O_2 concentration correlates remarkably well with the cell viability. Other species in the liquid like $^{\cdot}OH$ or superoxide anion radical ($O_2^{\cdot -}$) do not vary significantly with feed gas humidity.

Keywords: hydrogen peroxide, human skin cells, gas phase, plasma jet, humidity, liquid phase

1. Introduction

Applications in plasma medicine require not only an understanding of the plasma sources and the generated plasma but also demand information on the active agent transition from the gas into the liquid phase and finally their interaction with the cells. However, this is a complex task since an interdisciplinary approach as well as extended experimental and theoretical research is necessary. Large efforts have been made in the diagnostics and control of atmospheric pressure plasmas intended for biomedical applications [1–4]. Also, by the support of sophisticated theoretical models first insights into the complex nature of plasma cell and plasma liquid interactions were obtained [5–8]. The aim of those investigations is to uncover work mechanisms of the plasma. This goes along with the identification of dominant species which are generated by the plasma in the gas and/or liquid phase and have a significant influence on the biological sample [9]. For prokaryotic cells Pavlovich *et al* and Shimizu *et al* found a correlation between the ozone concentration produced by a dielectric barrier discharge (DBD) operated in air and the inactivation efficacy of *Escherichia coli* [10, 11]. The impact of ozone on bacteria is well known and many water disinfection facilities are based on DBDs [12, 13]. However,

that does not automatically mean that ozone is the dominant species in plasma medicine, where usually eukaryotic cells are plasma treated. Kalghatgi *et al* showed that DBD treatment of mammalian breast epithelial cells differ completely from pure ozone treatment, although ozone is one of the dominant plasma generated species in the gas phase [14]. They concluded that long living organic hydroperoxides mediate the DNA damaging effect of non-thermal plasma in mammalian cells. Haertel *et al* investigated the effect of DBD in argon and air on human skin cells (HaCaT keratinocytes) and observed that changes in integrin expression were related to intracellular reactive oxygen species (ROS) induction, while ozone has no influence [15]. Their study also discussed the dominant role of hydrogen peroxides (H_2O_2). Two years before, Sato *et al* already found that H_2O_2 is a key inactivation factor for HeLa cells treated by a pulsed corona discharge in air [16]. For a radio frequency driven atmospheric pressure argon plasma jet, Winter *et al* observed that increased feed gas humidity results in an elevated inhibition of indirectly treated HaCaT cells [17]. Interestingly, the gas phase ozone concentration generated under these experimental conditions showed an opposing trend and was thus not considered as the dominant species responsible for the observed cell effect. It was pointed out in this work that H_2O_2 in liquid phase increases with increasing feed gas humidity and a possible correlation with the cell response was discussed. Hydrogen peroxide was also identified as a central player in plasma-induced oxidative stress in human blood cells [18].

H_2O_2 is a quite important biologically relevant reactive species which can be detected throughout the human body. Peroxisomes and mitochondria show elevated levels as a by-product of mitochondrial respiration and β-oxidation of fatty acids, respectively [19–21]. Hydrogen peroxide is also an important mediator of wound healing processes, as it is secreted by epithelial cells after injuries have occurred, thereby initiating inflammatory processes [22]. In a similar setting, it is an effective antimicrobial means of innate immune cells (macrophages, neutrophils) upon the uptake of pathogens [23–25]. However, its omnipresence strongly requires control mechanisms to level the intra and extracellular H_2O_2 concentration. Many enzymes have evolved to that effect, the most efficient being catalase: one molecule of catalase readily transforms up to several million H_2O_2 molecules into water (H_2O) and oxygen (O_2) molecules every second [26]. Nevertheless, elevated levels or defective enzymes or detoxification pathways may cause serious damage to single cells or tissues, especially considering that it readily passes through cell membranes [19]. DNA damage has been described, from single base modifications to single and double strand breaks, as well as (per-) oxidation of (membrane) lipids (especially unsaturated lipids) and proteins leading to various cell changes, starting with mere modifications of cell shape and cytoskeleton to total loss of viability and disintegration of the cellular membrane [19, 20, 27–31]. Elevated levels of H_2O_2 are also considered to play an important role in the skin depigmentation disease Vitiligo [32].

Even though H_2O_2 is considered a mildly oxidizing species, it does not directly oxidize most biological molecules. It rather acts through its conversion to the highly reactive products hydroxyl radical ($^{\cdot}OH$) and hydroperoxyl radical ($HO_2^{\cdot}$), which can be formed by photodissociation of H_2O, by the decay of peroxynitrite/peroxynitrous acid ($O{=}NOO^-/O{=}N{-}OOH$) or by the Fenton reaction in the case of $^{\cdot}OH$ [33, 34].

The aim of the current study is to trace the H_2O_2 molecule from its plasma based generation in the gas phase to the liquid phase and show that H_2O_2 concentration correlates strongly with the inhibition of adherent human skin cells.

2. Materials and methods

2.1. Plasma jet

The plasma source, a cold atmospheric pressure plasma jet (kinpen, neoplas GmbH, Germany), used in this study is identical to the device used in the related study concerning the impact of feed gas humidity [17]. It consists of a centred rod electrode inside a ceramic capillary and a grounded ring electrode [35, 36]. The ceramic capillary has an inner and outer diameter of 1.5 mm and 2.5 mm, respectively. When a sinusoidal voltage signal of 2 to 6 kV_{pp} with a frequency of about 1 MHz is applied to the centred electrode, plasma is ignited within the core region of the jet and about a 10 mm long effluent becomes visible after ignition. The working gas was argon (Argon N50, Air Liquide) with a gas flow rate of 3 standard litres per minute (slm). In order to generate hydrogen peroxide by the plasma, the humidity concentration of the feed gas was changed by means of a bubbler setup exemplarily shown in figure 1. The feed gas humidification setting was similar to the setting used in [17]. The feed gas humidity was measured with a chilled mirror dew point hygrometer (DewMaster, EdgeTech, USA). For Fourier transformed infrared (FTIR) measurements the jet was equipped with a shielding gas device as reported in [37]. For details see section 2.3. All other plasma treatment results are performed without a shielding gas device.

2.2. Detection OH in the plasma jet effluent

The detection of gas phase hydroxyl radical density under atmospheric conditions by laser-induced fluorescence (LIF) is still under investigation and requires significant calibration efforts to yield absolute densities [38–41]. However, relative hydroxyl radical density is already interesting since basic information about chemistry dynamics can be concluded. In this work, the relative density of hydroxyl radicals is measured for different feed gas humidity settings by LIF using the P1(4) transition of the OH(A,X)(1,0) at 283.452 nm and chosen for its good absorption efficiency and its well isolated spectral position from neighbouring lines. The excitation is performed by a frequency doubled dye laser (Cobra Stretch, Sirah Laser und Plasmatechnik GmbH, Germany) pumped with a 10 Hz pulsed Nd : Yag laser (SpectraPhysics, Inc., USA). The LIF signal is transmitted through a 10 nm FWHM bandpass filter centred at 308 nm. The detection is performed by a photomultiplier tube (R5916U51, Hamamatsu, Japan) connected to a digital oscilloscope (DPO 4104, Tektronix Ltd.,

United Kingdom). The laser beam diameter is adjusted by a 500 μm aperture and not focused. The laser spot is pointed on-axis on the plasma effluent at 1.0 mm distance from the nozzle. In order to ensure a linear LIF response to the laser energy and to avoid saturation effects, a laser energy scan is performed. Consequently, the laser energy is set to 120 μJ per pulse. The LIF intensity I_{LIF} is known to be proportional to the laser energy I_L [39] and can be simplified in our case by:

$$I_{LIF} \propto \frac{n_{OH}}{\sum_i k_i \cdot n_i} \cdot I_L \quad (1)$$

where n_{OH} is the hydroxyl radical density, k_i the quenching and vibrational energy transfer (VET) coefficient and n_i is the density of a quencher species i which contributes to fluorescence losses. Argon from the feed gas, nitrogen and oxygen from the surrounding air and water from the admixture are the main quenchers of the fluorescence. However, it is a reasonable assumption to consider only water as a quencher since its density is a variable parameter, whereas argon, nitrogen and oxygen densities remain constant. The LIF signal is thus corrected from quenching and VET losses by using the following value reported in literature for water molecules, $k_{H_2O} = 6.6 \times 10^{-10}$ cm^3 s^{-1} [42].

2.3. Detection of H_2O_2 in plasma afterglow

FTIR spectroscopy is a broadband absorption technique that enables the detection and quantification of molecules absorbing in the infrared spectral region. Since gas phase H_2O_2 has significant absorption bands in the spectral range from 1200 to 1330 cm^{-1} FTIR spectroscopy is the method of choice to analyse H_2O_2 [43]. In this study an FTIR spectrometer (Vertex 70v, Bruker Optics GmbH, Germany) was equipped with an additional white type multipass cell (A134G/QV, Bruker Optics GmbH, Germany), which provides a total absorption length of 19.2 m. The pressure in the multipass cell was reduced to 100 mbar by means of a vacuum pump in order to prolong the lifetime of the plasma generated species and to reduce the distracting influence of ambient water and carbon dioxide (CO_2). Due to this low-pressure setting the atmospheric pressure plasma jet could not be operated directly in the multipass cell. Thus, the jet was equipped with a pressurized air flushed shielding gas device with a nozzle diameter of 5 mm, similar to the one reported in [37], and attached to an additional glass chamber as displayed in figure 1. The gas from the shielding (5 slm compressed and dried air) and from the jet (3 slm argon) flows into the glass chamber and exhausts via an outlet. Hence, the pressure in the glass chamber is slightly higher than the ambient (1020–1030 mbar). Furthermore, the glass chamber was connected to the multipass cell by means of an adjustable needle valve so that a small fraction of the gas flow was sampled continuously by the FTIR system. The gas flow rate through the multipass cell is 1.5 slm. The gas mixing and particle residence time in the glass chamber was calculated by computational fluid dynamics simulations in a previous work for an identical geometry setting [37]. It was shown that the majority of particles remain within the mixing cell for a few seconds before they enter the FTIR multipass cell. This means that highly reactive species have enough time to react and form long living products, like H_2O_2 or O_3, which were detected with the FTIR setup.

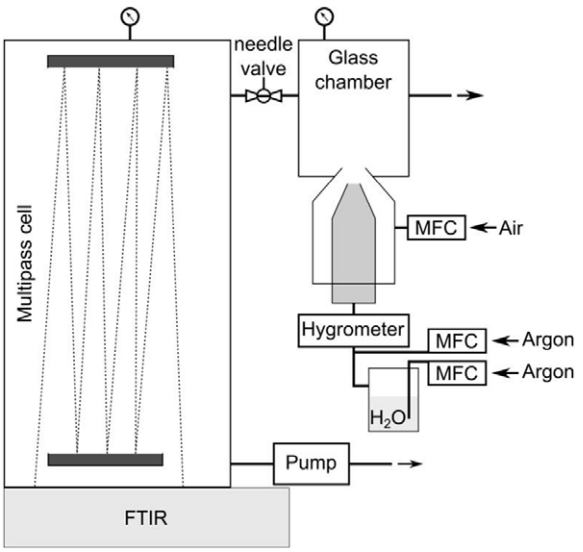

Figure 1. FTIR setup schematic for detecting H_2O_2 in the plasma jet downstream using FTIR spectroscopy combined with a multipass cell. MFC: mass flow controller.

In order to investigate the influence of feed gas humidity on the produced species the argon feed gas was humidified with the bubbler setup as displayed in figure 1. Before the FTIR measurement was performed the plasma jet was switched off while the particular gas mixture was flushed through the jet and the multipass cell. After 10 min the background signal was obtained. Subsequently, the jet was switched on. Several FTIR spectra were obtained for at least 10 min to validate the constant absorption band intensity. This proves a steady state measurement of species concentration in the multipass cell. The obtained spectra were fitted using fitting tool software (QMACSoft 1.1.3, neoplas control GmbH, Germany), that is based on the Hitran database and on the Levenberg–Marquardt algorithm [43, 44]. This allows for the identification of absorption bands as well as the calculation of species densities by applying Beer–Lambert's law to the measured optical depths. This measurement and evaluation procedure was performed for all humidity settings, so that an individual background signal was obtained for every humidity condition.

By replacing the humidifier bubbler by an identical vessel filled with 150 ml of 10% H_2O_2 solution, created by diluting a 30% H_2O_2 stock solution (9.7 M, Merck, Germany) and leaving everything else unaltered, gas phase H_2O_2 was generated without igniting the plasma. By varying the argon gas flow rate passing through the H_2O_2 bubbler the amount of gas phase H_2O_2 concentration was adjusted. The H_2O_2 concentration was determined analogue to the previously described procedure.

2.4. Plasma treatment of RPMI solution

As in the previous study [17], a volume of 5 mL complete cell growth medium (Roswell Park Memorial Institute RPMI

1640 + 8% fetal calf serum + 1% penicillin/streptomycin solution) filled in a polystyrene Petri dish (60 mm diameter TPP, Trasadingen, Switzerland) was plasma treated. The treatment time was varied between 0 and 100 s. During that treatment time the plasma jet was constantly moved in a meandering pattern over the Petri dish by means of a *xyz*-stepping motor. The distance between the nozzle and the liquid surface was 9 mm. During plasma treatment, the 3 slm argon gas flow rate leads to evaporation of the liquid. By measuring the remaining liquid volume after the longest treatment time (100 s), it was found that the initial 5 mL liquid volume misses 130 μl$\pm$10 μl. This evaporated liquid volume is only about 2.6% of the initial volume and is thus neglected in the H_2O_2 concentration evaluation.

By means of a thermometer the liquid temperature was measured before and after 100 s plasma treatment and no relevant temperature increase was observed.

2.5. Detection of reactive species concentrations in liquid cell growth medium

Hydrogen peroxide was measured with the test stripe method described in [17]. According to this method three times 30 μl of the plasma treated RPMI medium were sampled with a pipette directly after plasma treatment. These sample volumes were put onto three H_2O_2 test stripes (Merckoquant110011, Merck, Germany). After a waiting time of 60 s the test stripes were read out by a digital microscope camera (Conrad, Germany) in order to analyse their colour values. By comparing the obtained colour values with a calibration curve the H_2O_2 concentration was determined. This procedure was conducted three times so that finally nine test stripes were evaluated for every feed gas humidity setting investigated.

The same test stripe method was utilized for the H_2O_2 bubbler setup. For direct comparison the same H_2O_2 bubbler setup was used as for the FTIR measurements. In this experiment, the cell growth medium was exposed to the working gas flow for 40, 60 and 80 s without plasma ignition. The gas flow and treatment procedure is identical to the plasma treatment using humidified feed gas. By comparing the results of both experiments the effect of plasma for H_2O_2 production in liquid is investigated. The results are discussed in section 3.2.

Also the stability of plasma produced H_2O_2 in RPMI was investigated. Therefore, three H_2O_2 start concentrations of 0.8, 2.9 and 9.0 mg l^{-1} within a volume of 5 ml RPMI were produced via plasma treatment with three experimental settings, namely: dry argon gas and a treatment time of 20 or 180 s and with humidified argon (1660 ppm) and a treatment time of 80 s. Each setting was repeated three times. Subsequent to the plasma treatment the H_2O_2 concentrations in each Petri dish were measured at different times after plasma treatment applying the test stripe method described above. We intentionally did not use commercial H_2O_2 stock solution for the H_2O_2 life time experiments, since in contrast to plasma treated H_2O_2, it contains stabilizers. This would distort the results of the life time measurements in the RPMI solution.

The measurement of low H_2O_2 concentrations in the case of the dry feed gas for the purpose of cell viability

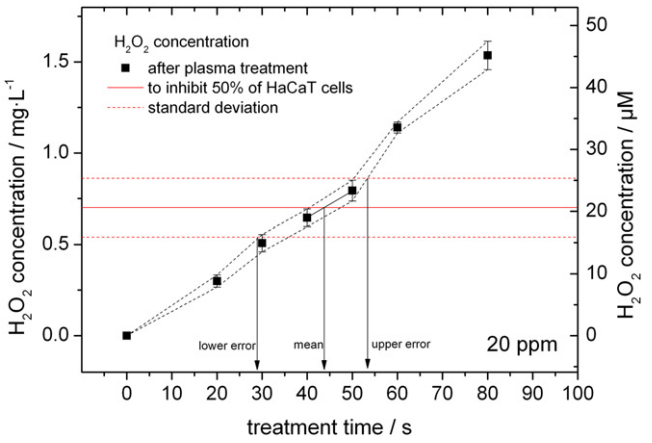

Figure 2. Method to obtain the H_2O_2 related inhibition time. The horizontal solid line depicts the H_2O_2 concentration that inhibits 50% of adherent HaCaT cells. This value was determined experimentally. Square dots are the measurement values for plasma generated H_2O_2 concentration in RPMI medium after different treatment times. The treatment time given by the interception point of both curves is the half inhibition treatment time, since the H_2O_2 concentration in the medium reaches the concentration to inhibit 50% of HaCaT cells. The dashed lines represent the error intervals of both measurements. From these lines the lower and upper error of the half inhibition treatment time were deduced.

comparison was performed by means of a homogeneous assay (Amplex Red Hydrogen Peroxide/Peroxidase Assay Kit, Invitrogen Ltd, USA). The assay was applied analogue to the method described in [17]. It is more sophisticated than the test stripe method but leads to a higher accuracy in H_2O_2 concentration determination. This is important for the correlation evaluation described in section 2.6 since errors made in H_2O_2 concentration measurement will directly affect the accuracy of the cell inhibition time determination (see figure 2).

The radical concentrations of hydroxyl ($^{\cdot}OH$) and superoxide anion ($O_2^{\cdot-}$) in cell growth medium for different feed gas humidity settings and a plasma treatment time of 40 s were measured by electron paramagnetic resonance (EPR) spectroscopy. The protocol applied in this work is described in [45]. Due to the short lifetime of these radicals in liquid spin traps, 5-tert-Butoxycarbonyl-5-methyl-1-pyrroline-N-oxide (BMPO, Dojindo Laboratoire, Japan) and 5,5-dimethy-1-pyrroline-N-oxide (DMPO, Dojindo Laboratoire, Japan) were used. DMPO was solved in the RPMI cell culture medium to a concentration of 100mM. This spin trap cannot distinguish between hydroxyl radicals ($^{\cdot}OH$) and superoxide anion radicals ($O_2^{\cdot-}$). BMPO on the other hand distinguishes between both species. However, until now we were not able to obtain an EPR signal from BMPO in RPMI. Thus, experiments with BMPO were conducted by solving 10mM of BMPO in Dulbecco's phosphate buffered saline (DPBS) solution instead of RPMI. Each EPR measurement was repeated three times.

Parallel to the above mentioned measurements the pH value of 40 s plasma treated RPMI solution was measured directly after plasma treatment using a pH meter (Sevenmulti M47, Mettler Toledo, Switzerland).

2.6. Relating H_2O_2 concentration to cell viability

To answer the question, whether plasma generated H_2O_2 correlates with the viability of indirectly treated adherent human keratinocytes (HaCaT cells), inhibition measurements are taken from figure 12 in [17]. This inhibition curve depicts how long a cell culture needs to be treated by the argon plasma jet at a certain feed gas humidity concentration in order to inhibit 50% of the cell metabolic activity. For instance, at completely dry conditions a plasma treatment duration of about 45 s is necessary to reach this inhibition level whereas at a significantly higher humidity concentration of 1250 ppm half the cells lose their viability already after a treatment time of 16 s. In order to relate H_2O_2 measurements with these data the inhibition concentration of H_2O_2 was determined. Therefore, the same HaCaT cell type was handled identically as in [17] with the difference that the cells were not covered with a plasma treated RPMI medium but with an RPMI medium containing different well defined H_2O_2 concentrations. These concentrations were produced by diluting 30% H_2O_2 stock solution (9.7 M, Merck, Germany) in RPMI. As a result, the H_2O_2 concentration to inhibit 50% of HaCaT cells was determined as $(21 \pm 4)\mu$M (solid horizontal line in figure 2, corresponding to $(0.71 \pm 0.14)\,\mathrm{mg\,l^{-1}}$). The uncertainty interval (horizontal dashed lines) is the standard deviation of 8 measurements.

Figure 2 also shows the increase of the H_2O_2 concentration in the RPMI cell growth medium for a plasma jet treatment with dry argon feed gas after different treatment times. From the intercept point of this curve with the solid horizontal line the half inhibition treatment time is deduced. At this time point of plasma treatment duration, the H_2O_2 concentration due to plasma treatment reaches 21μM and is as high as the H_2O_2 concentration to inhibit half of the HaCaT cells. Every plasma treatment that will produce this H_2O_2 level after a certain treatment time will inhibit at least half of the HaCaT cells. Moreover, if the treatment time to inhibit half of the HaCaT cells by plasma is similar to the time in which the H_2O_2 concentration due to the plasma treatment increased up to 21μM, then H_2O_2 plays the major role in modulating cellular activities.

The method to estimate the uncertainty of the half inhibition treatment time is also indicated in figure 2. The lower and upper error is obtained by evaluating the intercept points of the H_2O_2 inhibition concentration uncertainty and the error interval of the plasma generated H_2O_2 measurement.

3. Results and discussion

3.1. Generation of H_2O_2 in the gas phase

A FTIR spectrum of the exhaust argon jet plasma gas is presented in figure 3 for a feed gas humidity concentration of 1220 ppm together with the resulting fit curve. The most dominant absorption in this spectrum is given by H_2O_2. Furthermore, distinct absorption bands of ozone (O_3) were obtained. Both band structures, H_2O_2 and O_3, were fitted and their concentration in the multipass cell was calculated. For this particular humidity setting the concentration of H_2O_2

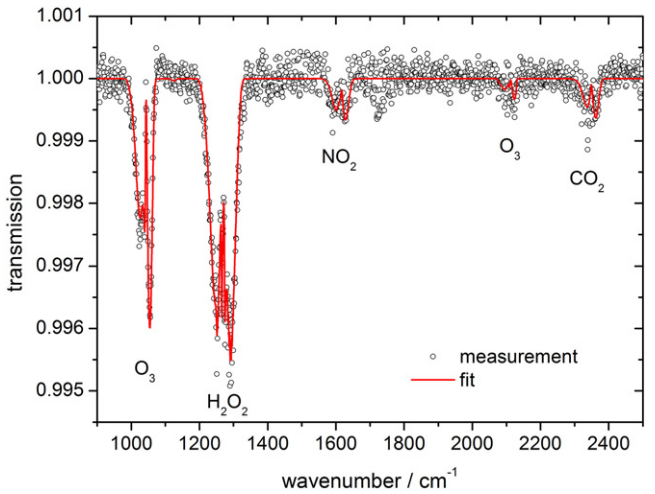

Figure 3. FTIR spectrum in the far field of an atmospheric pressure argon plasma jet for a feed gas humidity of 1220 ppm measured in a multipass cell with an absorption length of 19.2 m and a pressure of 100 mbar. Absorption bands of ozone, hydrogen peroxide, nitrogen dioxide and carbon dioxide were detected. The fit was performed by using the Hitran database. For clarity every fifth measurement point is shown.

and O_3 are 3.6 ppm and 2.0 ppm, respectively. Despite the long purging procedure and careful background acquisition CO_2 absorption bands originating from ambient impurities are detectable. The spectral range from 1350 to 1700 $\mathrm{cm^{-1}}$ is also influenced by ambient water absorption bands which influence the quantitative evaluation of other molecular absorption bands in that region. Even though nitrogen dioxide (NO_2) was also identified in the spectrum, it could not be evaluated quantitatively due to its small signal and the overlapping water bands.

Evaluating the H_2O_2 absorption band for every adjusted feed gas humidity value leads to the H_2O_2 concentration curve, which is displayed in figure 4(*a*). With increasing humidity in the argon feed gas the H_2O_2 concentration in the multipass cell rises from almost zero for dry feed gas condition to a concentration of 5.3 ppm for a humidity setting of 1800 ppm. Additional to the measurement results in figure 4(*a*) the result of a simulation, based on the far field chemical reaction simulation reported in [37], is plotted. From that simulation, relevant production and destruction reactions for H_2O_2 were obtained. However, since the model aims to simulate particle densities in the far field of the jet without considering electron processes, it is difficult to include H_2O_2 generation processes that occur in the plasma jets core, where electrons play a major role. With only H_2O and Ar present in the core zone H_2O_2 formation occurs by recombination of $^{\cdot}OH$ radicals that are previously created by particle impact dissociation of water molecules according to [46]

$$H_2O + P \rightarrow {}^{\cdot}OH + {}^{\cdot}H + P \qquad (2)$$

and

$${}^{\cdot}OH + {}^{\cdot}OH + M \rightarrow H_2O_2 + M, \qquad (3)$$

where P is an energetic particle from the plasma (e.g. electron or excited argon atom) and M is a collision partner (e.g. argon).

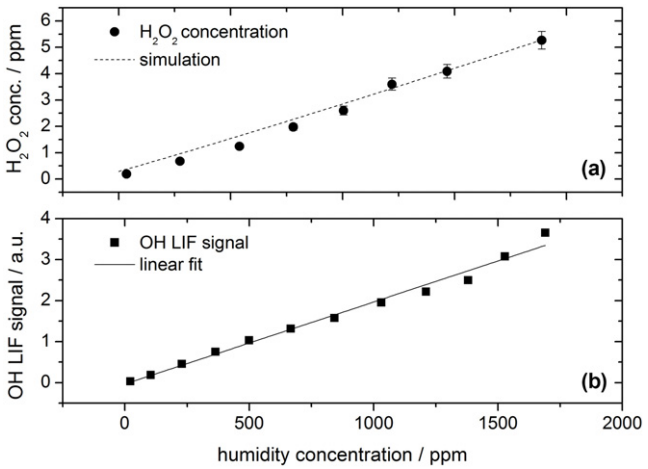

Figure 4. Results of absorption experiments in the gas phase. (*a*) H_2O_2 concentration in the multipass cell (far filed) and (*b*) relative LIF signal of the $^{\cdot}OH$ radical in dependence on the feed gas humidity (measured in plasma effluent). The $^{\cdot}OH$ LIF signal was fitted with a linear function whereas the dashed line in (*a*) is the simulation result.

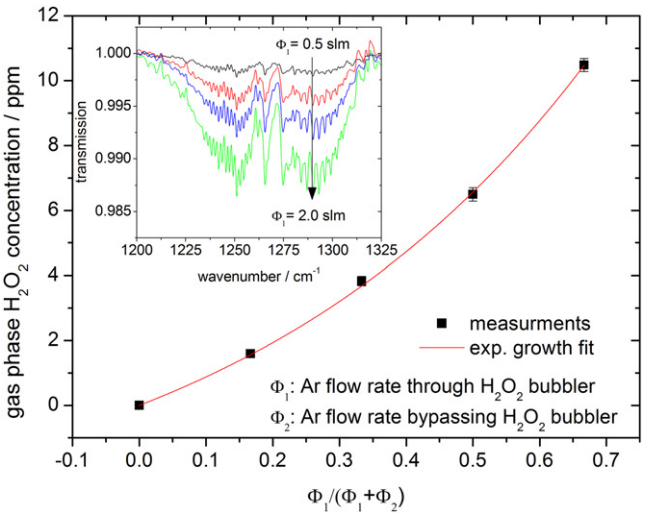

Figure 5. Gas phase H_2O_2 concentration increases as a consequence of higher argon flow rate through an H_2O_2 bubbler. No plasma is ignited in this experiment. As an inlay the FTIR transmission curves are given in the spectral range from 1200–1325 cm^{-1} for argon gas flow rates through the bubbler of 0.5, 1.0, 1.5 and 2.0 slm.

The dissociation process of equation (2) cannot directly be included into the simulation. Even so, by considering the almost linear slope of the measured relative $^{\cdot}OH$ density (see figure 4(*b*)) and by varying the degree of dissociation of H_2O as long as, under consideration of all included reactions, the simulated H_2O_2 profile fits with the measured one, this shortcoming can be avoided. The experimental based simulation predicts a linear increase of the far field H_2O_2 concentration with rising humidity. This result, together with positive simulation benchmarks on other experimental data [37], indicates that the most relevant equations for describing the production and destruction of H_2O_2 are considered within the simulation. The fact that a slight H_2O_2 concentration is predicted for zero feed gas humidity, results from the model assumption of a 36% relative ambient humidity.

H_2O_2 cannot only be produced in the core region of the plasma. In the effluent plasma region ambient species like O_2 diffuse into the plasma zone and influence the plasma chemistry. Thus, atomic hydrogen ($H^{\cdot}$) reacts with molecular oxygen to form hydroperoxyl radicals ($HO_2^{\cdot}$)

$$^{\cdot}H + O_2 + M \rightarrow HO_2^{\cdot} + M. \quad (4)$$

The combination of two of these radicals

$$2HO_2^{\cdot} + M \rightarrow H_2O_2 + O_2 + M \quad (5)$$

leads to the production of H_2O_2. As discussed in Reuter *et al* the electron density and temperature in the effluent region is lower compared to the situation in the core plasma region [47]. Furthermore, the educts $^{\cdot}OH$ and $HO_2^{\cdot}$, important for the production of H_2O_2, strongly react with each other to form water and oxygen and are thus not available for H_2O_2 production. Both effects make the effluent region less efficient for H_2O_2 production as experimentally shown in [47]. It was shown by the help of the simulation that other reactions to form H_2O_2, for instance via the reaction of water and ozone, play only a minor role.

Besides H_2O_2 generation by the argon plasma jet, gas phase H_2O_2 was alternatively created by bubbling a fraction of the argon feed gas through a reservoir of hydrogen peroxide solution. The amount of gas phase H_2O_2 was adjusted by the ratio of the argon feed gas flow rate that passes the H_2O_2 bubbler and the total argon flow rate of 3 slm. The H_2O_2 concentration in the gas phase produced by this method is displayed in figure 5. The measured H_2O_2 spectrum, on which the concentration determination is based, is also given in figure 5 (inlay) for different flow rates through the H_2O_2 bubbler. When the gas flow rate through the bubbler is increased, more H_2O_2 molecules are present in the gas phase and consequently the transmission of radiation in the FTIR multipass cell decreases. Evaluating these transmission curves yields a rising H_2O_2 concentration curve, which is zero for no bubbling and 10.5 ppm when an argon flow rate of 2 slm passes through the H_2O_2 bubbler. The produced H_2O_2 concentrations are in the same range as the concentrations produced by the argon plasma jet for different feed gas humidity settings. An exponential growth function resembles the H_2O_2 concentration curve quite well. This non-linear behaviour is due to the increased bubble size and turbulence within the H_2O_2 bubbler with increasing gas flow rate, which leads to an increased interaction surface between the gas and liquid phases. This results in an increased amount of H_2O_2 molecules in the gas passing through the bubbler. Together with the rising mixing ratio of this H_2O_2 bubbled gas and the unbubbled gas, a disproportionate gas phase H_2O_2 concentration is obtained.

3.2. Transition of gas phase H_2O_2 into liquid phase

H_2O_2 can be generated in plasma treated liquids in different ways. Either it is created inside the liquid by plasma induced liquid chemistry processes or gas phase H_2O_2 is dissolved in the liquid. In the first case plasma generated agents like energetic radiation or particles transfer energy from the gas to

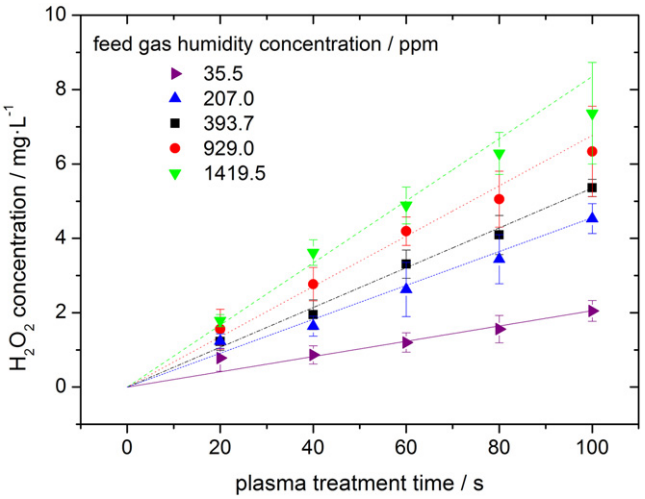

Figure 6. Increase of H_2O_2 concentration in 5 ml RPMI cell growth medium with plasma treatment time and for different feed gas humidity settings. The measurement was performed with colorimetric assays. The linear curves are results from linear regression.

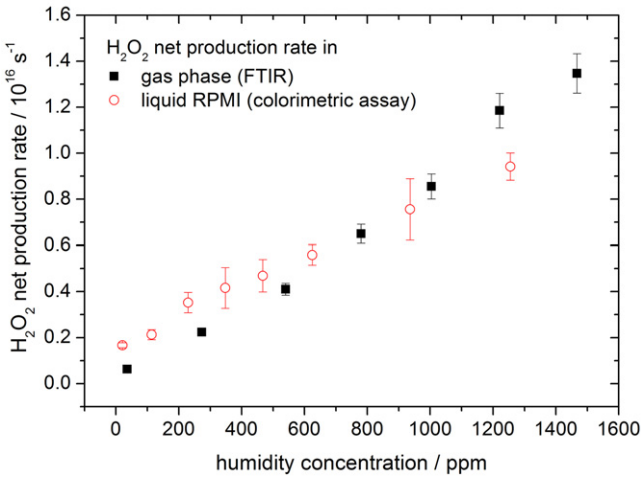

Figure 7. Net production rate of H_2O_2 molecules in the gas and liquid phase for different feed gas humidity settings.

the liquid phase and initiates the production of an ·OH radical within the liquid. Two of these radicals can recombine to form H_2O_2.

If the solubility process dominates, a correlation between H_2O_2 production in the gas and liquid phase must exist. Therefore, the H_2O_2 net production rate P_g in s^{-1} in the gas phase is calculated from the measured concentrations c in ppm in the multipass cell according to

$$P_g = c \cdot 2.47 \times 10^{19}\,\mathrm{cm}^{-3} \cdot (\Phi_1 + \Phi_2) \cdot 16.\bar{6}\,\mathrm{cm}^3\,\mathrm{s}^{-1}\,\mathrm{slm}^{-1}, \quad (6)$$

where Φ_1 and Φ_2 are the feed gas flow rate (3 slm) and the curtain gas flow rate (5 slm), respectively. The factor 16.6 is due to the unit conversion of standard litre per minute into the SI unit cm^{-3} s^{-1}. The calculation of H_2O_2 net production rate P_L in the liquid cell growth medium is done by

$$P_L = \frac{A \cdot V_L \cdot N_A \cdot 10^{-3}}{M} \quad (7)$$

assuming a linear increase A (in mg l^{-1} s^{-1}) of H_2O_2 concentration with time. V_L in L is the volume of the treated medium, N_A is the Avogadro constant and M in g mol^{-1} is the molar mass of H_2O_2. According to figure 6, where the increase of H_2O_2 concentration in RPMI is displayed for different feed gas humidity settings, the assumption of a linear H_2O_2 increase with time is quite reasonable due to the good agreement of the measured values and the linear regression curves.

Figure 7 shows the result of the H_2O_2 net production rate determinations of the gas and liquid phases for different feed gas humidity settings. Interestingly, both curves are in a remarkable agreement.

This means that the H_2O_2 net production rate in the gas and liquid phases are identical for the investigated humidity conditions and implies that the presence of H_2O_2 molecules in the gas phase directly influences the liquid phase H_2O_2 concentration. Although this positive correlation is not proving that liquid phase H_2O_2 molecules originate from gas phase H_2O_2, at least it is strong evidence that in our experiment solubility processes play a major role in generating H_2O_2 in liquid.

In order to find further evidence for this indication an additional experiment was performed. If solubility processes determine the H_2O_2 concentration in plasma treated cell growth medium, then a simple non-plasma argon gas flow through the jet nozzle, containing the same H_2O_2 molecule density (in the multipass cell of the FTIR) as was generated by the humidified plasma jet, must result in the same liquid H_2O_2 concentration. In a first approximation, it is assumed that the H_2O_2 concentration above the liquid is identical for both the plasma generated and the bubbler produced H_2O_2. If plasma has a direct H_2O_2 production effect in addition to solubility processes on the cell growth medium, then the H_2O_2 concentration in the liquid will be higher for the plasma case than for the non-plasma case. As described in section 2, the non-plasma H_2O_2 generation was performed by using a H_2O_2 bubbler. The gas phase H_2O_2 concentrations for the plasma-on case (humidified argon gas) and for the H_2O_2 bubbler are taken from figures 4(*a*) and 5, respectively.

The results of this study are depicted in figure 8 for three different treatment times. With a rising H_2O_2 amount in the gas phase, the liquid phase H_2O_2 concentration increases. This general trend is independent whether the gas phase H_2O_2 is created by the plasma jet or by a H_2O_2 bubbler without any plasma. However, the resulting liquid phase H_2O_2 concentration is slightly higher for the plasma case. Especially for the longest investigated treatment time of 80 s, more liquid phase H_2O_2 is generated by the plasma jet than with the H_2O_2 bubbler at comparable gas phase H_2O_2 densities. Returning to the argumentation above, this discrepancy means that additional to the solubility of gas phase H_2O_2 in the liquid the plasma itself has a direct contribution to the liquid phase H_2O_2 amount. Thus, the hypothesis that entirely all hydrogen peroxide found in the liquid medium results from a solubility process of gas phase H_2O_2, is falsified. The amount of this direct plasma contribution, however, is smaller than the effect obtained by the H_2O_2 bubbler. On average, more than 60 % of

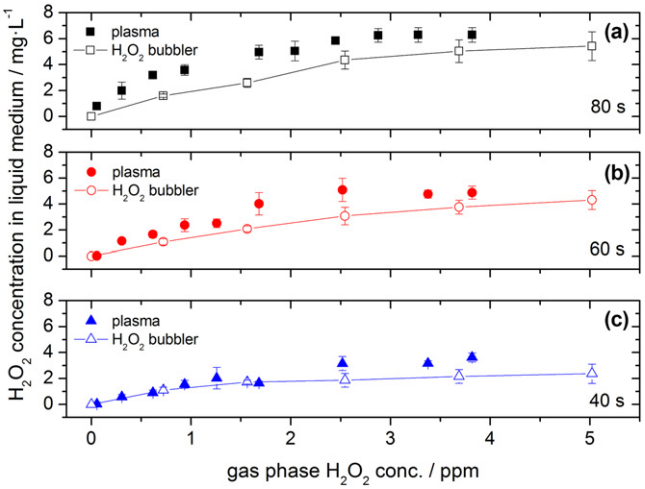

Figure 8. Influence of gas phase H_2O_2 on the H_2O_2 concentration in liquid medium. The RPMI cell growth medium was treated (*a*) 80 s, (*b*) 60 s or (*c*) 40 s by the argon plasma jet (full symbols) and by a non-plasma condition, where an argon gas flow was enriched with H_2O_2 molecules originating from a H_2O_2 bubbler (line connected open symbols). The corresponding gas phase H_2O_2 concentrations were obtained in the FTIR multipass cell (see figures 4(*a*) and 5) and do not represent the H_2O_2 concentration above the RPMI solution.

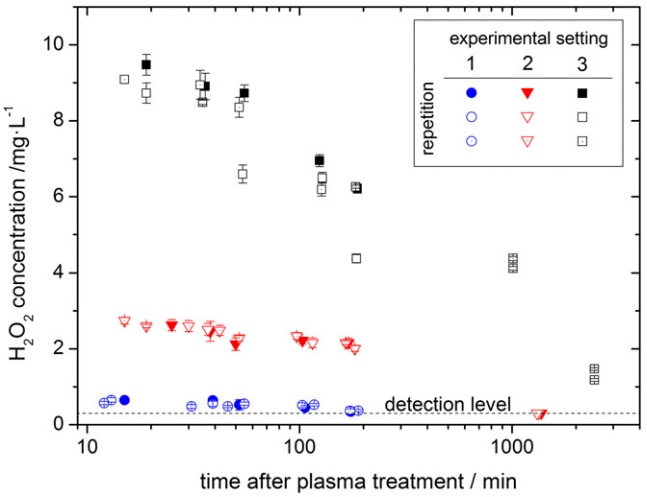

Figure 9. Stability of plasma produced H_2O_2 in RPMI medium in dependence of the time after the plasma treatment has finished. Experimental settings were: (1) feed gas humidity: <20 ppm, treatment time: 40 s, (2) feed gas humidity: <20 ppm, treatment time: 180 s, (3) feed gas humidity: 1660 ppm, treatment time: 80 s.

Table 1. Henry's constants at standard conditions for inorganic species present in gas or liquid phase in the current study.

Species	Henry's constant (mol l^{-1} Pa^{-1})	Reference
Oxygen (O_2)	1.2×10^{-8}	[49]
Argon (Ar)	1.4×10^{-8}	[50]
Nitrogen (N_2)	6.5×10^{-8}	[51]
Ozone (O_3)	1.1×10^{-7}	[52]
Nitrogen dioxide (NO_2)	4.0×10^{-7}	[53]
Hydroxyl radical ($^{\cdot}OH$)	2.9×10^{-4}	[54]
Hydroperoxyl radical ($HO_2^{\cdot}$)	4.0×10^{-2}	[55]
Hydrogen peroxide (H_2O_2)	8.3×10^{-1}	[56]

the liquid phase H_2O_2 was generated without direct plasma effect. Thus, the solubility of gas phase H_2O_2 plays an important role for the generation of liquid phase H_2O_2—at least in our experimental setup.

The question, why the H_2O_2 solubility process is so dominant, is answered when comparing Henry's constant for solubility of different species (see table 1). According to Henry's law the concentration of a species in aqueous solution is proportional to its partial pressure over the liquid [48]. The proportionality factor is Henry's constant. The higher the value of this constant, the better molecules dissolve into the liquid. Compared to argon or oxygen Henry's constant is more than 7 orders of magnitude higher for H_2O_2. In fact, H_2O_2 has one of the highest Henry's constants compared with other inorganic species. Hence, a gas phase H_2O_2 molecule in proximity to an aqueous solution will most likely enter it.

3.3. Stability of plasma generated H_2O_2 in RPMI

In principle, to have an effect on adherent cells the H_2O_2 molecule or its decomposition products must live long enough to reach the cells or be produced by post-plasma treatment reactions. Possible decomposition products like $^{\cdot}OH$ or $O_2^{\cdot-}$ have an extremely short lifetime. In biological systems the hydroxyl radical has a lifetime in the nanosecond and the superoxide anion radical in the microsecond range [57]. Thus, to be effective they must be produced in direct proximity to the cell molecule to be attacked. Compared to this, the lifetime of plasma generated H_2O_2 is quite long as the measured data in figure 9 depict. As described in section 2.5 three different H_2O_2 starting concentrations were produced by plasma treatment. Afterwards the degradation of the plasma generated H_2O_2 was determined. For the first half hour after plasma treatment the H_2O_2 concentration stayed almost unchanged, independent of the concentration reached directly after the plasma treatment. However, after a sufficient period of time the concentration decreases. For the highest starting value the H_2O_2 concentration in the RPMI medium decreases from 9 down to 1.5 mg l^{-1} after 2000 min. No H_2O_2 concentration was measurable for the lower starting concentrations after that time. A possible reason for this decay is the decomposition of H_2O_2 via the Fenton reaction, since the cell growth medium contains iron.

When performing this H_2O_2 life time experiment with H_2O_2 from stock solution that contains stabilizers, the concentration decrease is much lower. Within 120 h the H_2O_2 concentration decreases from an initial concentration of 10 to 6.7 mg l^{-1} (data not shown). For long time experiments this different behaviour of stock solution H_2O_2 and plasma generated H_2O_2 must be considered.

3.4. H_2O_2 correlates with inhibition of HaCaT cells

In figure 10, the half inhibition treatment time for different feed gas humidity settings is displayed for indirect plasma treatment (data taken from [17]) and for the case that the cell inhibition effect is based on H_2O_2 only. The data for

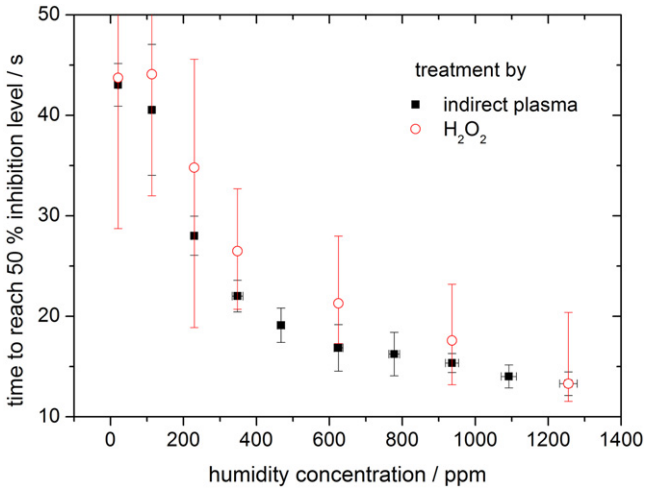

Figure 10. Time to reach 50% cell inhibition for different feed gas humidity concentrations. The results of indirect plasma treatment (data taken from [17], treatment time of the medium: 40 s) and for the case that H_2O_2 is the only agent agree remarkably well.

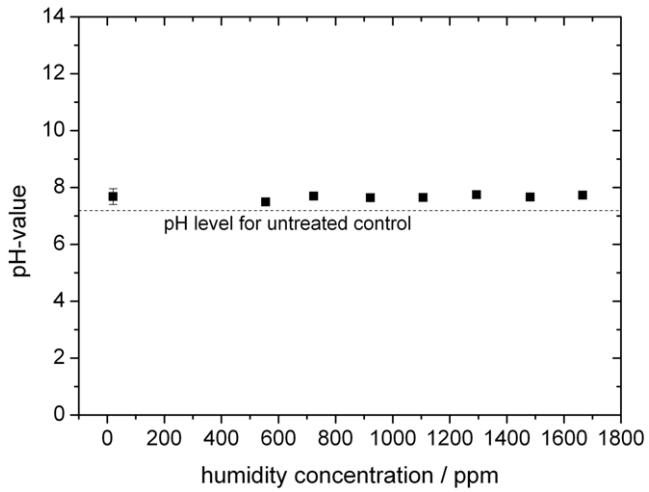

Figure 11. pH-value measured in RPMI after 40 s plasma treatment time for different feed gas humidity settings. The squares are the measurements after plasma treatment. The dashed line depicts the pH-value for the untreated control.

the latter is determined according to the procedure described in section 2.6. It is obvious that the effect of H_2O_2 not only follows the cell viability decrease but is almost identical to the effect that originates from plasma treatment. This means that for our treatment conditions H_2O_2 plays a dominant role for the inhibition of indirectly plasma treated HaCaT cells in RPMI cell growth medium. Whether this role has a direct H_2O_2 impact on the cells or is due to the impact of its decomposition products cannot be answered with this data. Either way, the amount of H_2O_2 produced within the liquid determines the viability of the cells. A similar effect of H_2O_2 on viability of human thyroid epithelial cells (HTori-3) was found by Marinov *et al* using a water discharge setup [58, 59].

Looking closer to the results in figure 10 the average time to reach the 50% inhibition level is slightly higher for the H_2O_2 case, which would mean that besides the H_2O_2 impact other agents must contribute to the cell inhibition. Owing to the large error bars the significance of this finding is debatable. However, to ensure the dominance of H_2O_2 measurements of pH-value and of $^{\cdot}OH$ and $O_2^{\cdot-}$ radical concentrations were also conducted.

Figure 11 shows the results for the pH-value. For different feed gas humidity settings no severe change in pH is observed and thus a contribution of pH to the cell inhibition is excluded. This was expected since the used cell growth medium is buffered. Only a general slightly elevated pH level is found when comparing the plasma treated values with the untreated control. This is due to a degassing effect [60]. During plasma treatment, the RPMI cell growth medium is strongly swirled by the feed gas flow and thus previously chemically bound CO_2 evaporates from the liquid. Since dissolved CO_2 can form carbonic acid within the liquid a lack of CO_2 leads to a more alkaline condition.

The radical concentrations for $^{\cdot}OH$ and $O_2^{\cdot-}$ in a plasma treated DPBS medium are shown in figure 12. With rising feed gas humidity little change in the radical concentration is observed. At most a slight decrease is detected. The $^{\cdot}OH$ and $O_2^{\cdot-}$ radical concentrations are between 0.2–0.3μM and 0.45–0.65μM, respectively. The observation that both concentrations do not increase with feed gas humidity implies two conclusions. Firstly, their production in the bulk medium is not directly or dominantly linked to the produced H_2O_2 concentration which itself increases with increasing feed gas humidity. If a direct link would exist the radicals are expected to resemble the H_2O_2 trend. Since this is not the case the radical production must be generated due to other plasma agents. Secondly, the bulk concentrations of $^{\cdot}OH$ and $O_2^{\cdot-}$ do not contribute directly to the inhibition of the investigated adherent HaCaT cells. However, since the measured concentrations are volume averaged values it might well be that directly at the cells the radical concentrations are quite inhomogeneous. Thus, their concentration might be much higher close to the cells than what is measured in the bulk medium.

It has to be mentioned that the presented EPR measurements were not performed in an RPMI medium, but in a DPBS medium while the other measurements were performed in RPMI. As discussed in section 2.5 this was due to the lack of signal obtained with the BMPO spin trap in RPMI. The spin trap BMPO is to be preferred since with it $^{\cdot}OH$ and $O_2^{\cdot-}$ radicals can be distinguished, whereas the spin trap DMPO only provides the sum of both radical densities. DMPO on the other hand was used in RPMI. In order to verify that the constant behaviour of both radicals with respect to the feed gas humidity is not only a DPBS specific observation the experiment was repeated in RPMI with a DMPO spin trap. The comparison of both measurements yielded that whether the sum of $^{\cdot}OH$ and $O_2^{\cdot-}$ density is obtained with BMPO in DPBS or with DMPO in RPMI the trends of both curves are identical (data not shown). Even the absolute concentrations are in good agreement. The combined radical concentration of $^{\cdot}OH$ and $O_2^{\cdot-}$ is only by a factor of less than two higher for the measurements of DMPO in RPMI. Thus, the results obtained in DPBS with the spin trap BMPO are transferable to the RPMI medium and are therefore relevant for the cell and H_2O_2 measurements performed in RPMI.

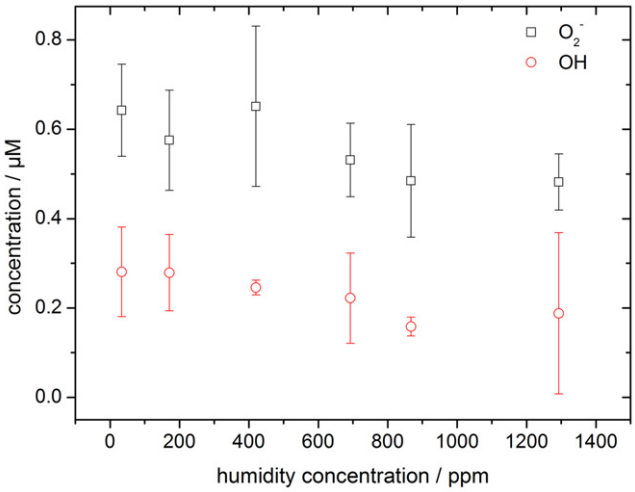

Figure 12. Radical concentrations of superoxide $O_2^{\cdot-}$ and hydroxyl $^{\cdot}OH$ obtained by EPR spectroscopy in DPBS for different feed gas humidity concentrations. The plasma treatment time was 40 s.

Concluding this section, it was shown that plasma produced H_2O_2 correlates positively with the inhibition of adherent human skin cells. The concentrations of $^{\cdot}OH$ and $O_2^{\cdot-}$ do not depend on the feed gas humidity and therefore do not correlate with the observed cell inhibition effect. As expected for the buffered cell growth medium no influence of pH value was detected. In the following it is discussed whether these findings can be generalized and what their impact for plasma medicine actually is.

Whenever H_2O_2 is generated by plasma treatment in a liquid medium it will affect human skin cells (as was shown in this work) and other cell types within this medium (as described in the introduction). However, the implication that H_2O_2 correlates in every case with an observed effect on cells and is therefore the only relevant agent in plasma medicine is not the correct conclusion. It was shown by Barton *et al* and Tresp *et al* with a similar plasma source that the viability of HaCaT cells, as well as of a monocyte cell line (THP-1), changes significantly when altering the nitrogen to oxygen surrounding gas ratio, while the H_2O_2 concentration in the medium stayed almost unchanged [61, 62]. Taking these results into account a more differentiated picture evolves. The strong role of H_2O_2 concerning cell viability is observable especially when the plasma parameter variation leads to a severe change of H_2O_2 concentration, as it is the case for feed gas humidity alteration. In other cases, where the resulting H_2O_2 level is zero or invariant against parameter variation, other effects on top of the H_2O_2 effect become visible. Hence, H_2O_2 is a quite an important molecule in plasma medicine concerning cell activity but not the only one.

4. Conclusion

In this work, the pathway of hydrogen peroxide was followed from its generation in the gas phase by a humidified argon atmospheric pressure plasma jet into liquid cell culture medium. For this, FTIR and LIF spectroscopy were applied to measure the gas phase H_2O_2 concentration and the relative $^{\cdot}OH$ radical density in dependence of the feed gas humidity level. By means of an adapted far field simulation the most important production and destruction mechanisms of H_2O_2 were identified for the given experimental conditions. In the presented case, H_2O_2 is mainly produced inside the core plasma zone by the dissociation of water molecules. The resulting $^{\cdot}OH$ radicals recombine to form H_2O_2.

By comparing the H_2O_2 net production rate in the gas and liquid phase a remarkable compliance was found. Moreover, by mimicking the H_2O_2 generation of the plasma jet with the help of an H_2O_2 bubbler it is concluded that the solubility of gas phase H_2O_2 plays a major role in generating hydrogen peroxide in the liquid. This finding is explained by the high Henry's constant of H_2O_2 compared to other present species.

The stability of this plasma generated and dissolved H_2O_2 was measured in the cell growth medium to exceed half an hour without changing. After 40 h however, almost no H_2O_2 was detected in the medium. Besides the physical and chemical focus on H_2O_2, its effect on the viability of adherent human skin cells was investigated. Pure plasma generated H_2O_2 has the similar effect on the cell viability than indirect plasma treatment. This finding was ensured by analysing the pH-value and liquid-borne radical densities of $^{\cdot}OH$ and $O_2^{\cdot-}$ by EPR spectroscopy. Neither of those agents showed a significant dependence on the feed gas humidity variation. Hence, no correlation with cell viability is expected for bulk concentrations of these agents. This leaves H_2O_2 as the dominant species for our experimental conditions. Since experiments are known and discussed in this work where a variation of a biological marker does not correlate with H_2O_2 it is concluded that H_2O_2 is a quite important molecule in plasma medicine but not the only one.

Acknowledgments

This work is funded by German Federal Ministry of Education and Research (grant# 03Z2DN11 & 03Z2DN12). The authors thankfully acknowledge the valuable work of Liane Kantz, Sebastian Schlegel, Mattis Hänel, Sven Bordewick and Johannes von Saß.

References

[1] von Woedtke T, Reuter S, Masur K and Weltmann K D 2013 Plasmas for medicine *Phys. Rep.* **530** 291–320
[2] Laroussi M 2009 Low-temperature plasmas for medicine *IEEE Trans. Plasma Sci.* **37** 714–25
[3] Fridman G, Friedman G, Gutsol A, Shekhter A B, Vasilets V N and Fridman A 2008 Applied plasma medicine *Plasma Process. Polym.* **5** 503–33
[4] Kong M G, Kroesen G, Morfill G, Nosenko T, Shimizu T, van Dijk J and Zimmermann J L 2009 Plasma medicine: an introductory review *New J. Phys.* **11** 115012
[5] Babaeva N Y and Kushner M J 2013 Reactive fluxes delivered by dielectric barrier discharge filaments to slightly wounded skin *J. Phys. D: Appl. Phys.* **46** 025401
[6] Tian W, Norberg S, Babaeva N Y and Kushner M J 2013 The interaction of atmospheric pressure plasma DBDs and jets with liquid covered tissues: fluxes of reactants to underlying cells *Proc. 21st Int. Symp. Plasma Chemistry (Cairns)*

[7] Bruggeman P and Leys C 2009 Non-thermal plasmas in and in contact with liquids *J. Phys. D: Appl. Phys.* **42** 053001
[8] Yusupov M, Neyts E C, Simon P, Berdiyorov G, Snoeckx R, van Duin A C T and Bogaerts A 2014 Reactive molecular dynamics simulations of oxygen species in a liquid water layer of interest for plasma medicine *J. Phys. D: Appl. Phys.* **47** 025205
[9] Graves D B 2012 The emerging role of reactive oxygen and nitrogen species in redox biology and some implications for plasma applications to medicine and biology *J. Phys. D: Appl. Phys.* **45** 263001
[10] Pavlovich M J, Chang H-W, Sakiyama Y, Clark D S and Graves D B 2013 Ozone correlates with antibacterial effects from indirect air dielectric barrier discharge treatment of water *J. Phys. D: Appl. Phys.* **46** 145202
[11] Shimizu T, Sakiyama Y, Graves D B, Zimmermann J L and Morfill G 2012 The dynamics of ozone generation and mode transition in air surface micro-discharge plasma at atmospheric pressure *New J. Phys.* **14** 103028
[12] Kogelschatz U, Eliasson B and Egli W 1997 Dielectric-barrier discharges. Principle and applications *J. Phys. IV France* **7** 47–66
[13] Ehlbeck J, Schnabel U, Polak M, Winter J, von Woedtke T, Brandenburg R, von dem Hagen T and Weltmann K D 2011 Low temperature atmospheric pressure plasma sources for microbial decontamination *J. Phys. D: Appl. Phys.* **44** 013002
[14] Kalghatgi S, Fridman A, Azizkhan-Clifford J and Friedman G 2012 Damage in mammalian cells by non-thermal atmospheric pressure microsecond pulsed dielectric barrier discharge plasma is not mediated by ozone *Plasma Process. Polym.* **9** 726–32
[15] Haertel B, Straßenburg S, Oehmigen K, Wende K, von Woedtke T and Lindequist U 2013 Differential influence of components resulting from atmospheric-pressure plasma on integrin expression of human HaCaT keratinocytes *BioMed Res. Int.* **2013** 761451
[16] Sato T, Yokoyama M and Johkura K 2011 A key inactivation factor of HeLa cell viability by a plasma flow *J. Phys. D: Appl. Phys.* **44** 372001
[17] Winter J, Wende K, Masur K, Iseni S, Dünnbier M, Hammer M U, Tresp H, Weltmann K D and Reuter S 2013 Feed gas humidity: a vital parameter affecting a cold atmospheric-pressure plasma jet and plasma-treated human skin cells *J. Phys. D: Appl. Phys.* **46** 295401
[18] Bekeschus S, Kolata J, Winterbourn C, Kramer A, Turner R, Weltmann K D, Broker B and Masur K 2014 Hydrogen peroxide: a central player in physical plasma-induced oxidative stress in human blood cells *Free Radical Res.* **48** 542–9
[19] Halliwell B and Cutteridge J M C 1999 *Free Radicals in Biology and Medicine* (Oxford: Clarendon)
[20] Chance B, Sies H and Boveris A 1979 Hydroperoxide metabolism in mammalian organs *Physiol. Rev.* **59** 527–605
[21] de Groot H and Littauer A 1989 Hypoxia, reactive oxygen, and cell injury *Free Radical Biol. Med.* **6** 541–51
[22] Niethammer P, Grabher C, Look A T and Mitchison T J 2009 A tissue-scale gradient of hydrogen peroxide mediates rapid wound detection in zebrafish *Nature* **459** 996–9
[23] Aderem A and Underhill D M 1999 Mechanisms of phagocytosis in macrophages *Annu. Rev. Immunol.* **17** 593–623
[24] Bogdan C, Röllinghoff M and Diefenbach A 2000 Reactive oxygen and reactive nitrogen intermediates in innate and specific immunity *Curr. Opin. Immunol.* **12** 64–76
[25] Dahlgren C and Karlsson A 1999 Respiratory burst in human neutrophils *J. Immunol. Methods* **232** 3–14
[26] Lisanti M P, Martinez-Outschoorn U E, Lin Z, Pavlides S, Whitaker-Menezes D, Pestell R G, Howell A and Sotgia F 2011 Hydrogen peroxide fuels aging, inflammation, cancer metabolism and metastasis *Cell Cycle* **10** 2440–9
[27] Imlay J A and Linn S 1988 DNA damage and radical toxicity *Science* **240** 1302–9
[28] Jaruga P and Dizdaroglu M 1996 Repair of products of oxidative DNA base damage in human cells*Nucleic Acid Res.* **24** 1389–94
[29] Hinshaw D B, Sklar L A, Bohl B, Hyslop P A, Rossi M W and Spragg R G 1986 Cytoskeletal and morphologic impact of cellular oxidant injury *Am. J. Pathol.* **123**
[30] Simon R H, Scoggin C H and Patterson D 1981 Hydrogen peroxide causes the fatal injury to human fibroblasts exposed to oxygen radicals *J. Biol. Chem.* **256** 7181–6
[31] Weiss S J, Young J, LoBuglio A F, Slivka A and Nimeh N F 1981 Role of hydrogen peroxide in neutrophil-mediated destruction of cultured endothelial cells*J. Clin. Invest.* **68** 714–21
[32] Hasse S, Gibbons N C J, Rokos H, Marles L K and Schallreuter K U 2004 Perturbed 6-tetrahydrobiopterin recycling via decreased dihydropteridine reductase in vitiligo: more evidence for H_2O_2 stress *J. Invest. Dermatol.* **122** 307–13
[33] Ueda J, Saito N, Shimazu Y and Ozawa T 1996 A comparison of scavenging abilities of antioxidants against hydroxyl radicals *Arch. Biochem. Biophys.* **333** 377–84
[34] Hampton M B and Orrenius S 1997 Dual regulation of caspase activity by hydrogen peroxide: implications for apoptosis *FEBS Lett.* **414** 552–6
[35] Weltmann K D, von Woedtke T, Hähnel M, Stieber M and Brandenburg R 2010 Atmospheric-pressure plasma sources: prospective tools for plasma medicine *Pure Appl. Chem.* **82** 1223–37
[36] Reuter S, Winter J, Iseni S, Peters S, Schmidt-Bleker A, Dünnbier M, Schäfer J, Foest R and Weltmann K D 2012 Detection of ozone in a MHz argon plasma bullet jet *Plasma Sources Sci. Technol.* **21** 034015
[37] Schmidt-Bleker A, Winter J, Iseni S, Dünnbier M, Weltmann K D and Reuter S 2014 Reactive species output of a plasma jet with shielding gas device—combination of FTIR absorption spectroscopy and gas phase modelling *J. Phys. D: Appl. Phys.* **47** 145201
[38] Dilecce G and De Benedictis S 2011 Laser diagnostics of high-pressure discharges: laser induced fluorescence detection of OH in He/Ar–H_2O dielectric barrier discharges *Plasma Phys. Control. Fusion* **53** 124006
[39] Verreycken T, van der Horst R M, Sadeghi N and Bruggeman P J 2013 Absolute calibration of OH density in a nanosecond pulsed plasma filament in atmospheric pressure He–H_2O: comparison of independent calibration methods *J. Phys. D: Appl. Phys.* **46** 464004
[40] Voráč J, Dvořák P, Procházka V, Ehlbeck J and Reuter S 2013 Measurement of hydroxyl radical (OH) concentration in an argon RF plasma jet by laser-induced fluorescence *Plasma Sources Sci. Technol.* **22** 025016
[41] Verreycken T, Mensink R, Horst R v d, Sadeghi N and Bruggeman P J 2013 Absolute OH density measurements in the effluent of a cold atmospheric-pressure Ar–H_2O RF plasma jet in air *Plasma Sources Sci. Technol.* **22** 055014
[42] Williams L R and Crosley D R 1996 Collisional vibrational energy transfer of OH ($A\,^2\Sigma^+$, $v' = 1$) *J. Chem. Phys.* **104** 6507
[43] Rothman L S *et al* 2005 The HITRAN 2004 molecular spectroscopic database *J. Quant. Spectrosc. Radiat. Transfer* **96** 139–204
[44] Zimmermann H 2010 QMACSoft-HT (computer program)
[45] Tresp H, Hammer M U, Winter J, Weltmann K D and Reuter S 2013 Quantitative detection of plasma-generated radicals in

liquids by electron paramagnetic resonance spectroscopy *J. Phys. D: Appl. Phys.* **46** 435401
[46] Bruggeman P and Schram D C 2010 On OH production in water containing atmospheric pressure plasmas *Plasma Sources Sci. Technol.* **19** 045025
[47] Reuter S, Winter J, Iseni S, Schmidt-Bleker A, Dünnbier M, Masur K, Wende K and Weltmann K D 2014 The influence of feed gas humidity versus ambient humidity on atmospheric pressure plasma jet-effluent chemistry and skin cell viability *IEEE Trans. Plasma Sci.* in press
[48] Sander R 1999 *Compilation of Henry's Law Constants for Inorganic and Organic Species of Potential Importance in Environmental Chemistry* Version 3 www.henrys-law.org
[49] Carpenter J H 1966 New measurements of oxygen solubility in pure and natural water *Limnol. Oceanogr.* **11** 264–77
[50] Morrison T J and Johnstone N B 1954 Solubilities of the inert gases in water *J. Chem. Soc.* 3441–6
[51] Wilhelm E, Battino R and Wilcock R J 1977 Low-pressure solubility of gases in liquid water *Chem. Rev.* **77** 219–62
[52] Kosak-Channing L F and Helz G R 1983 Solubility of ozone in aqueous solutions of 0–0.6M ionic strength at 5–30 °C *Environ. Sci. Technol.* **17** 145–9
[53] Lee Y-N and Schwartz S E 1981 Reaction kinetics of nitrogen dioxide with liquid water at low partial pressure *J. Phys. Chem.* **85** 840–8
[54] Berdnikov V M and Bazhin N M 1970 Oxidation–reduction potentials of certain inorganic radicals in aqueous solutions *Russ. J. Phys. Chem.* **44** 395–8 English translation
[55] Hanson D R, Burkholder J B, Howard C J and Ravishankara A R 1992 Measurement of OH and HO_2 radical uptake coefficients on water and sulfuric acid surfaces *J. Phys. Chem.* **96** 4979–85
[56] O'Sullivan D W, Lee M, Noone B C and Heikes B G 1996 Henry's law constant determinations for hydrogen peroxide, methyl hy-droperoxide, hydroxymethyl hydroperoxide, ethyl hydroperoxide, and peroxyacetic acid *J. Phys. Chem.* **100** 3241–7
[57] Pryor W A 1986 Oxy-radicals and related species: their formation, lifetimes, and reactions *Ann. Rev. Physiol.* **48** 657–67
[58] Marinov I and Rousseau A 2013 personal communication
[59] Marinov I 2013 Plasmas in contact with liquids and at the interfaces. Application for living cell treatment *PhD Thesis* Paris, France: École Polytechnique, Laboratoire de Physique des Plasmas
[60] Buxton G V and Elliot A J 1986 Rate constant for reaction of hydroxyl radicals with bicarbonate ions *Int. J. Radiat. Appl. Instrum.* C **27** 241–3
[61] Barton A, Wende K, Bundscherer L, Weltmann K D, Lindequist U and Masur K 2013 Non-thermal atmospheric pressure plasma treatment of human cells: the effect of ambient conditions *Proc. 21st. Int. Symp. Plasma Chem. (Cairns)*
[62] Tresp H, Hammer M U, Weltmann K D, Winter J and Reuter S 2014 Effects of atmosphere composition and liquid type on plasma generated reactive species in biologically relevant solutions *Plasma Med.* in press